Biochimica et Biophysica Acta, 470 (1977) 58—69

BBA 77802

MISCIBILITY PROPERTIES OF BINARY PHOSPHATIDYLCHOLINE MIXTURES

A CALORIMETRIC STUDY

P.W.M. VAN DIJCK, A.J. KAPER, H.A.J. OONK [a] and J. DE GIER

Biochemical Laboratory and [a] *"Chemical Thermodynamics Group", State University of Utrecht, Transitorium III, Padualaan 8, University Centre "De Uithof", Utrecht (The Netherlands)*

(Received January 27th, 1977)

Summary

From data obtained by differential scanning calorimetry phase diagrams were constructed, using a thermodynamically based fitting method. The following binary mixtures of phosphatidylcholines in water were studied: 14:0/14:0-glycerophosphocholine/16:0/16:0-glycerophosphocholine, 14:0/14:0-glycerophosphocholine/18:0/18:0-glycerophosphocholine, 12:0/12:0-glycerophosphocholine/16:0/16:0-glycerophosphocholine, $18{:}1_t/18{:}1_t$-glycerophosphocholine/14:0/14:0-glycerophosphocholine and $18{:}1_t/18{:}1_t$-glycerophosphocholine/16:0/16:0-glycerophosphocholine.

A comparison is made of the present results with those obtained using probe techniques and the differences are discussed.

Introduction

Miscibility properties of two components can be described by a phase diagram. From the shape of the fluid-solid region conclusions can be drawn with respect to the miscibility of two substances both in the solid state and in the fluid state; therefore it is important to measure accurately the temperature region in which there is a coexistence of solid and fluid material.

In model membrane systems water is present as well as the phospholipid components, so actually a ternary system is studied when working with binary mixtures of phospholipids. However, influences of water are neglected in fully hydrated binary phospholipid systems. Most phase diagrams published for binary phospholipid mixtures are interpretations of data obtained by probe techniques [1—4]. A disadvantage of a probe technique is the assumption that the probe does not disturb the local organization and reflects the exact situation of the bulk phospholipids. Therefore, it is important to check the miscibility properties with the aid of a direct physical technique such as differential

scanning calorimetry. In fact the first phase diagrams [5] and some more recently reported phase diagrams [6,8] were derived from calorimetric data.

It is useful to extend these direct investigations with respect to the miscibility properties of mixtures of phospholipids because of the increasing number of reports using model membrane systems consisting of phospholipid mixtures. In this report we show that some precautions are needed before calorimetric data can be used for the construction of phase diagrams.

Materials and Methods

1,2-Dilauroyl-*sn*-glycero-3-phosphocholine (12:0/12:0-glycerophosphocholine), 1,2-dielaidyl-*sn*-glycero-3-phosphocholine ($18{:}1_t/18{:}1_t$-glycerophosphocholine), 1,2-dimyristoyl-*sn*-glycero-3-phosphocholine (14:0/14:0-glycerophosphocholine, 1,2-dipalmitoyl-*sn*-glycero-3-phosphocholine (16:0/16:0-glycerophosphocholine) and 1,2-distearoyl-*sn*-glycero-3-phosphocholine (18:0/18:0-glycerophosphocholine) were synthesized by Mrs. A. Lancée-Hermkens according to the method described by van Deenen and de Haas [9].

Samples were prepared for differential scanning calorimetry and measured as described before [10] with the modification which will be described in the results section. As the occurrence of a pretransition in synthetic phosphatidylcholines would interfere with an accurate determination of the temperature of the main transition in mixtures showing solid-solid immiscibility, the dispersion buffer consisted of 25 mM Tris/acetate/ethyleneglycol (1 : 1, v/v), 100 mM NaCl, pH 7.0. Under these conditions the phospholipid pretransition is absent. The intercept of the predominant slope of the first transition peak with the baseline will be taken as the solidus and fluidus point in heating and cooling scans respectively. At least three heating and three cooling scans were performed on each mixture. The deviation in the determination of both points was strongly dependent on the nature of the components and the ratio in which they were present in the mixture.

Freeze fracturing electron-microscopy was performed as described before [11].

Results

Calorimetric data

The most detailed phase diagram, derived from both ESR and differential scanning calorimetry data, is that of 14:0/14:0-glycerophosphocholine and 16:0/16:0-glycerophosphocholine [1,3—5,8] which approximates ideal mixing behaviour. For that reason we attempted to construct a phase diagram from calorimetric heating and cooling scans of various mixtures of 14:0/14:0-glycerophosphocholine and 16:0/16:0-glycerophosphocholine obtained at the usual scanning rate of 5° C per min. An example of such a heating scan is shown in Fig. 1a. Scanning of the pure components and mixtures yielded enough points to construct a phase diagram. However, from these points (Fig. 2) one would conclude that in the region of 10—35 mol% of 16:0/16:0-glycerophosphocholine solid-solid immiscibility occurs and this is in disagreement not only with all literature data on these lipid mixtures [1,3—5,8] but also with the fact

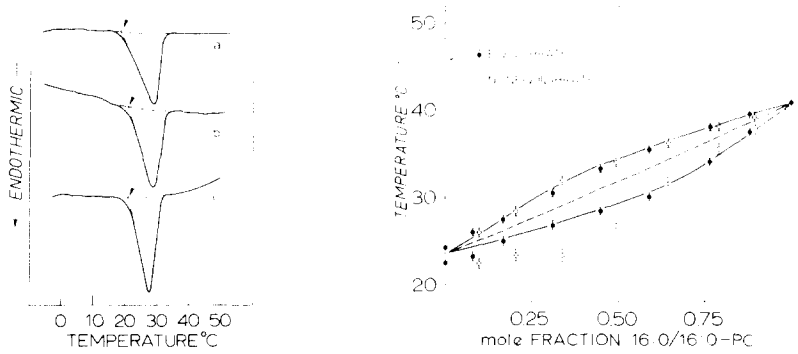

Fig. 1. Calorimetric heating scans of equimolar mixtures of 14:0/14:0-glycerophosphocholine/16:0/16:0-glycerophosphocholine using different experimental conditions. a: Reproducible heating scan obtained with a scanning rate of 5°C/min; cooling rate 5°C/min. b: Heating scan obtained at 5°C/min after cooling the sample at a rate of 0.31°C/min. c: First heating scan obtained at 5°C/min after an overnight incubation at 4°C.

Fig. 2. Phase diagram for 14:0/14:0-glycerophosphocholine/16:0/16:0-glycerophosphocholine (PC) with equal-*G* curve. The experimental points (○) were derived from scans obtained at heating and cooling rates of 5°C/min (compare Fig. 1a). The solidus points were obtained as the intersections of the slope of the descending arm of the endothermic heating curve with the baseline. The liquidus points represent the intersections of the slope of the ascending arm of the exothermic cooling curve with the baseline. The second set of data (●) was obtained from scans at scanning rates of 5°C/min. The heating scan was taken after an overnight preincubation at 4°C (compare Fig. 1c). The cooling scan was obtained immediately after the heating scan. The dotted line represents the equal-*G* curve.

that all 14:0/14:0-glycerophosphocholine/16:0/16:0-glycerophosphocholine mixtures display only 1 calorimetric peak.

Scanning through the transition at 5°C per min creates a non-equilibrium, which can be concluded from the fact that the end of the heating curve does not coincide with the beginning of the cooling curve and vice versa. This did not affect our measurements as we determined the solidus and liquidus points only from the beginning of the cooling and heating curve respectively. The only condition which has to be fullfilled in this case is that the interval between each scan through the transition region will leave enough time for the sample to equilibrate either in the liquid crystalline or in the gel state as the sagged solidus line is indicative for non-equilibrium conditions in the region of 10–50 mol% of 16:0/16:0-glycerophosphocholine. To obtain equilibrium data two approaches were followed: lowering the cooling rate and, as the apparatus allowed only a minimum cooling rate of 0.3°C/min, prolonged incubations below the transition region. The heating rates were in all cases kept at 5°C/min. Decreasing the cooling rate led to an ultimate increase of 3°C at the lowest scanning rate possible (0.3°C/min) (Fig. 1b). With prolonged incubation times in the gel state we could reach a higher value (4°C higher than under the original conditions of Fig. 1a). It appeared that an overnight incubation was necessary to yield a peak which did not change with respect to transition temperature and peak width upon longer preincubations (Fig. 1c). This preincubation period also led to an ultimate value in all other mixtures tested. The transition temperature, obtained after prolonged incubation in the gel state was higher

than the one obtained after cooling at 0.3°C/min. This implies that scanning at 0.3°C/min (20°C/h) gives a departure from equilibrium. Taking the end of a cooling scan, obtained at 10°C/h, as the solidus point as is often done in probe studies, is only permitted when it can be shown that this point coincides with the beginning of the heating curve. As the transition temperature in a cooling scan did not change either with lower scanning speed (in the previous heating scan) or prolonged equilibration in the liquid-crystalline state it can be concluded that, under these conditions, equilibration is very fast. As the time for reequilibration in the liquid-crystalline state was in the order of minutes one has to conclude that the lateral diffusion coefficient for phospholipid molecules in the liquid-crystalline state differs dramatically from that for molecules in the gel state. Cullis has shown recently that 16:0/16:0-glycerophosphocholine molecules in the liquid-crystalline state are at least 10 times more mobile than when they are in the gel state [12]. From our results it can be concluded that the difference, at least in binary mixtures, is even larger.

Thermodynamic description

Equal-G curve. In order to add significance to the experimental data we present the result of a thermodynamic interpretation based on the method of the equal-G curve [12]. The principles of that method will be outlined first, because they may be of particular value for the interpretation of biochemical phase diagrams.

The Gibbs energy of a solution, formed by $(1 - X)$ mol of the first component and X mol of the second, is, at constant pressure, usually given as

$$g(T, X) = (1 - X)\mu_1^* + X\mu_2^* + RT\{(1 - X)\ln(1 - X) + X \ln X\} + g^E(T, X) \qquad (1)$$

where T is the absolute temperature and R the gas constant. The first two terms with the Gibbs energies of the pure components (asterisks are used to refer to pure components) represent the Gibbs energy of the unmixed state. The third is the contribution due to ideal mixing. The last term, the excess Gibbs energy, gives the deviation from ideal-solution behaviour.

For each of the two phases such an expression can be given. At fixed temperature each of the functions corresponds to a curve in the gX-plane. On passing the temperature region in which the heterogeneous equilibrium takes place these two curves pass one another; at any intermediate temperature the coexisting phases are given by the points of contact of the common tangent, see Fig 3. The two sets of points of contact, obtained in this way, are the solidus and liquidus curves of the phase diagram. A third curve which can be plotted in the TX-plane is the equal-G curve; the set of points of intersection. It is clear that the equal-G curve always lies between the solidus and the liquidus curves.

Thermodynamic interpretation, i.e. the derivation of excess functions from phase diagrams, can be based on equilibrium curves, as well as on the equal-G curve. The interpretation based on equilibrium curves goes via thermodynamic potentials; it requires highly accurate data and is therefore hardly applicable to other than liquid-vapour equilibrium data. The equal-G curve (EGC) method, on the contrary, which is less dependent on experimental accuracy, is particularly useful to the equilibria studied here.

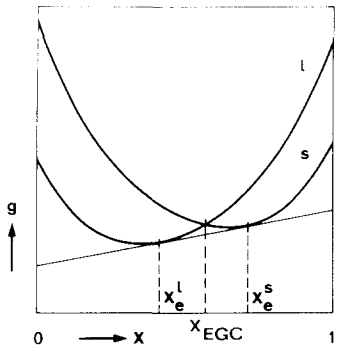

Fig. 3. Curves of the Gibbs energy versus the mol fraction for the solid (s) and liquid (l) state. The coexisting phases are given by the points of contact of the common tangent. EGC, equal-G curve.

Making use of the general relationship between Gibbs energy G, enthalpy H and entropy S, which is $G = H - TS$ and accordingly $\mu^* = h^* - Ts^*$ and $g^E = h^E - Ts^E$, Eqn. 1 yields the following two expressions for liquid (l) and solid (s) phase:

$$g^l = (1-X)h_1^{*l} + Xh_2^{*l} - T\{(1-X)s_1^* + Xs_2^{*l}\} + RT\{(1-X)\ln(1-X) + X\ln X\} + h^{El} - Ts^{El} \quad (2)$$

$$g^s = (1-X)h_1^{*s} + Xh_2^{*s} - T\{(1-X)s_1^{*s} + Xs_2^{*s}\} + RT\{(1-X)\ln(1-X) + X\ln X\} + h^{Es} - Ts^{Es} \quad (3)$$

$$\text{EGC}: (1-X)\Delta h_1^* + X\Delta h_2^* - T\{(1-X)\Delta s_1^* + X\Delta s_2^*\} + \Delta h^E - T\Delta s^E = 0$$

The equal-G curve which is the solution of

$$\Delta g = g^l - g^s = 0 \quad (4)$$

is given by

$$T_{EGC}(X) = \frac{(1-X)\Delta h_1^* + X\Delta h_2^* + \Delta h^E(X)}{(1-X)\Delta s_1^* + X\Delta s_2^* + \Delta s^E(X)} \quad (5)$$

In this equation Δh_1^* and Δh_2^* are the heats of melting and Δs_1^* and Δs_2^* are the entropies of melting of the first and second component, respectively (note that $\Delta h_1^* = T_{o1}\Delta s_1^*$ and $\Delta h_2^* = T_{o2}\Delta s_2^*$, where T_{o1} and T_{o2} are the melting points of the pure components 1 and 2).

The curve corresponding to Eqn. 5 with $\Delta h^E = 0$ and $\Delta s^E = 0$ is called zero line. (see Fig. 6.)

In the interpretation of solid-liquid equilibria of limited accuracy it is common practice to put the excess entropies of the phases equal to zero. In that case Δs^E vanishes from the denominator of the right-hand side of Eqn. 5. As a consequence, the temperature distance from zero line to equal-G curve is equal

to the quotient of difference excess enthalpy (the difference between the heats of mixing of both phases) divided by the entropy of melting.

Choice of excess function

For the excess enthalpy we use a two-parameter function which has proved to be very useful in the interpretation of phase diagrams with regions of demixing that are not symmetrical with respect to $X = \frac{1}{2}$ [14]. This function is of the form $(1 - X)^n X$ in which n is a positive number greater than 1.

The maximum of the form is at $1/(n + 1)$ and has the value $n^n/(n + 1)^{(n+1)}$. Multiplying the form with the reciprocal of the value of its maximum gives an expression the maximum of which has the value 1. The complete excess function we use is then

$$h^E(X) = A\{(n + 1)^{(n+1)}/n^n\}(1 - X)^n X \tag{6}$$

The constant A, which gives the value of the maximum, is a measure for the magnitude of the function and the exponent n is a measure for its asymmetry.

Interpretation

Thermodynamic interpretation of phase diagrams in this model means finding the values for A and for n for both of the participating phases. For the sake of simplicity we assume that for the systems studied here the value of n for the solid phase is equal to the value of n for the liquid phase. In that approximation the expression for the equal-G curve (EGC), Eqn 5, putting $\Delta A = A^l - A^s$, becomes

$$T_{EGC}(X) = \frac{(1 - X)\Delta h_1^* + X\Delta h_2^* + \Delta A\{(n + 1)^{(n+1)}/n^n\}(1 - X)^n X}{(1 - X)\Delta s_1^* + X\Delta s_2^*} \tag{7}$$

The procedure is now as follows. In the TX phase diagram a curve is drawn between liquidus and solidus which is expected to be a good representative of the real equal-G curve. From that curve the values of ΔA and n are obtained with the help of Eqn. 7, which may be rewritten as

$$T_{EGC}(X) = T_{ZERO}(X) + \frac{\Delta A\{(n + 1)^{(n+1)}/n^n\}(1 - X)^n X}{(1 - X)\Delta s_1^* + X\Delta s_2^*} \tag{8}$$

In the case of the system $18{:}1_t/18{:}1_t$-glycerophosphocholine/14:0/14:0-glycerophosphocholine (see Fig. 6), the drawn equal-G curve yielded the value 1.5 for n and the value -130 cal $\cdot$ mol^{-1} for ΔA; $T_{o1} = 284$ K, $T_{o2} = 296.5$ K, the values of the heats of melting being given in Table I. The solidus and liquidus curves shown in Fig. 6 were next calculated putting $A^l = 0$, i.e. assuming ideal behaviour in the liquid state, and with $A^s = A^l - \Delta A = +130$ cal $\cdot$ mol^{-1}. The result is in satisfactory agreement with the experimental data. At this place it may be noted that a phase diagram is more sensitive to a small change in ΔA than to relatively great changes in A^l and A^s with fixed ΔA. In the case of the system considered here, equally satisfactory agreement with the experimental data will be obtained by putting, e.g., $A^l = 50$ and $A^s = 180$ cal mol^{-1}, the difference with the diagram shown in Fig. 6 being a broadening of the two-phase region.

In most practical cases the best agreement is found by successive approxima-

TABLE I

THE VALUES OF THE HEATS OF MELTING

Mixture	Δh_1^*	Δh_2^*	n	A^l	A^S	Type of phase diagram *
	kcal · mol^{-1}	kcal · mol^{-1}		cal · mol^{-1}	cal · mol^{-1}	
14 : 0/14 : 0-glycerophosphocholine 16 : 0/16 : 0-glycerophosphocholine	6.8	8.6	1.0	125	150	[O]
12 : 0/12 : 0-glycerophosphocholine 16 : 0/16 : 0-glycerophosphocholine	4.3	8.6	1.65	75	250	[P]
14 : 0/14 : 0-glycerophosphocholine 18 : 0/18 : 0-glycerophosphocholine	6.8	10.7	1.65	100	275	[P]
18 : 1_t/18 : 1_t-glycerophosphocholine 14 : 0/14 : 0-glycerophosphocholine	7.3	6.8	1.5	0	130	[–]
18 : 1_t/18 : 1_t-glycerophosphocholine 16 : 0/16 : 0-glycerophosphocholine	7.3	8.6	1.2	150	255	[P]/[O] **

* Classification according to ref. 15

** See text.

tion, starting from equal-G curve and, e.g., putting $A^1 = 0$. During the calculations it may appear that the course of the equal-G curve needs a correction (some aspects of phase diagram calculations can be found in ref. 13).

For systems with limited miscibility in the solid state the values of A^1, A^s and n can be found with higher accuracy because, in terms of the model used, the region of demixing in the solid state is fully determined by A^s and n [14]. The following are some of the characteristics. With fixed n the critical temperature of mixing T_c, is proportional to A^s; some values for $A^s(n+1)^{(n+1)}n^{-n}/RT_c$ are 2.000 for $n = 1$, 2.130 for $n = 2$, 2.159 for $n = 4$. The mol fraction of the critical point, X_c, is determined by n alone:

$$X_c = \frac{(2n+1) - (2n^2-1)^{1/2}}{(n+1)^2} \tag{9}$$

In the case of the system 12:0/12:0-glycerophosphocholine/16:0/16:0-glycerophosphocholine the mean value of the coexisting solid phases is about 0.375, see Fig. 5. Assuming that this is also the value of X_c, the value of 1.65 is obtained for n. (Eqn. 9.) Next, the value of A^s is determined by successive approximation: in the case of demixing within one state the G-curve for that state is no longer convex over the whole mol-fraction region; the coexisting phases are given by the points of contact of the double tangent. For the system considered here the value which is found for A^s is 250 cal mol^{-1}. The value for A^1 is thereafter found by successive solidus and liquidus calculations, starting from an A^1 value derived from the estimated equal-G curve and the value found for A^s.

Application of this method (fitting data summarized in Table I) to the calorimetric data yielded the phase diagrams in Figs. 2, 4—7. The phase diagrams of the mixtures 14:0/14:0-glycerophosphocholine/16:0/16:0-glycerophosphocho-

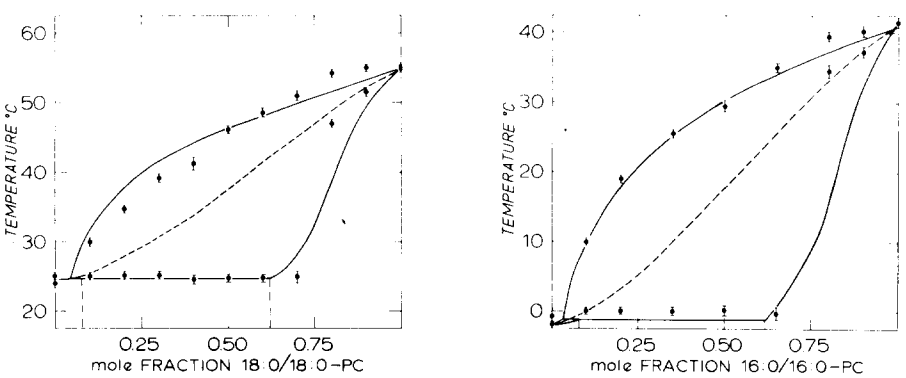

Fig. 4. Phase diagram for 14:0/14:0-glycerophosphocholine/18:0/18:0-glycerophosphocholine. Data were obtained as described in the legend of Fig. 2 for the second set of data (preincubation temperature 4°C). The dotted line is the equal-G curve.

Fig. 5. Phase diagram for 12:0/12:0-glycerophosphocholine/16:0/16:0-glycerophosphocholine. Data were obtained as described in the legend of Fig. 2 for the second set of data. (The samples were preincubated overnight at —15°C in the calorimeter). The dotted line is the equal-G curve.

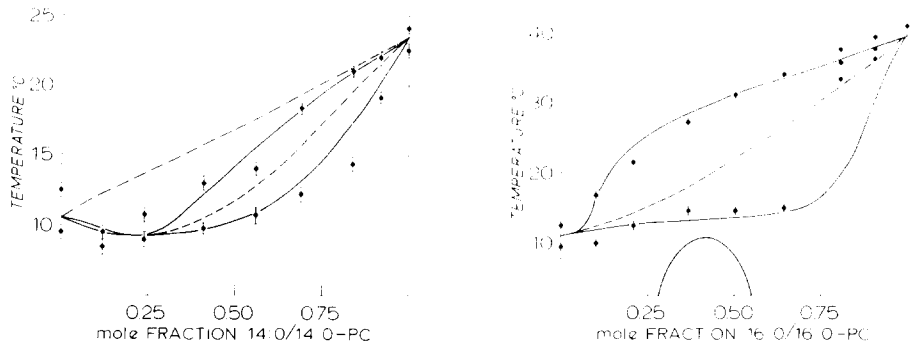

Fig. 6. Phase diagram for $18{:}1_t/18{:}1_t$-glycerophosphocholine/14:0/14:0-glycerophosphocholine. Data were obtained as described in the legend of Fig. 2 for the second set of data. (Preincubation overnight at 4°C in the calorimeter). Equal-G curve, (- - - - -); zero line, (· — · — ·).

Fig. 7. Phase diagram for $18{:}1_t/18{:}1_t$-glycerophosphocholine/16:0/16:0-glycerophosphocholine. Data were obtained as described in the legend of Fig. 2 for the second set of data. (Preincubated overnight at 4°C in the calorimeter). The dotted line is the equal-G curve.

line (Fig. 2) and $18{:}1_t/18{:}1_t$-glycerophosphocholine/14:0/14:0-glycerophosphocholine (Fig. 6) indicate that both components are miscible over the whole range and that in the latter case a minimum exists at about 25 mol% 14:0/14:0-glycerophosphocholine. The mixtures 12:0/12:0-glycerophosphocholine/16:0/16:0-glycerophosphocholine (Fig. 4), 14:0/14:0-glycerophosphocholine/18:0/18:0-glycerophosphocholine (Fig. 5), and $18{:}1_t/18{:}1_t$-glycerophosphocholine/16:0/16:0-glycerophosphocholine (Fig. 7) represent systems with a limited solid state miscibility. The system of $18{:}1_t/18{:}1_t$-glycerophosphocholine/16:0/16:0-glycerophosphocholine may be a mixture with a behaviour between limited and total miscibility in the solid state. We also have classified the phase diagrams in Table I.

From the data in Table I it has to be noted that although all A^l and A^s values are in the same range (the data for $18{:}1_t/18{:}1_t$-glycerophosphocholine and 14:0/14:0-glycerophosphocholine have to be taken only relative to each other) dramatic differences in shape and interpretation of the diagrams exist.

Discussion

In this paper we have modified the scanning calorimetric approach of constructing phase diagrams in such a way that it meets the objections to the technique of non-equilibrium conditions at the start of the phase transition due to the high scanning speed.

The results of our measurements show that one has to be very careful in interpreting data in terms of a phase diagram. The interpretation which has recently been given by Mabrey and Sturtevant [8] for the mixture of 14:0/14:0- and 18:0/18:0-glycerophosphocholine emphasizes the necessity to replace hand-drawn phase diagrams thermodynamically fitted phase diagrams. Using our method the data of Mabrey and Sturtevant could lead to a diagram with a miscibility gap in the gel phase from 15 to 70 mol% of 18:0/18:0-glycerophosphocholine and this, in contrast to their hand drawn

interpretation, would be in agreement not only with our diagram (Fig. 4) but also with earlier reported diagrams [2,4,5]. The diagrams of the mixtures 14:0/14:0-glycerophosphocholine/16:0/16:0-glycerophosphocholine, 12:0/12:0-glycerophosphocholine/16:0/16:0-glycerophosphocholine and 14:0/14:0-glycerophosphocholine/18:0/18:0-glycerophosphocholine are in qualitative agreement with diagrams reported before but with respect to mixtures in which $18:1_t/18:1_t$-glycerophosphocholine is one of the components both the shape and the interpretation of the diagrams are basically different from the diagrams previously published [2].

We conclude that $18:1_t/18:1_t$-glycerophosphocholine is perfectly miscible with 14:0/14:0-glycerophosphocholine, but that around 25 mol% of 14:0/14:0-glycerophosphocholine a mixture with a minimum transition temperature is formed (Fig. 6). In contrast, the probe data [2] have been interpreted to indicate complete solid-solid immiscibility up to 80 mol% 14:0/14:0-glycerophosphocholine. Our interpretation is supported by the following arguments:

1. At all ratios studied the mixture shows one homogeneous peak.

2. Electron microscopic analysis of an equimolar $18:1_t/18:1_t$-glycerophosphocholine/14:0/14:0-glycerophosphocholine mixture (Fig. 8a) quenched from 0°C reveals one homogeneous band pattern which is not identical with that for either of the pure components.

3. In the probe study [2] the transition temperature of pure $18:1_t/18:1_t$-glycerophosphocholine was taken as being infinitely sharp although in the experimental part a range of 10.5—13.5°C was mentioned. In mixtures the complete transition range was used. Furthermore no mixtures were studied between 0 and 25 mol% 14:0/14:0-glycerophosphocholine so the shape of the diagram is uncertain in this region.

Also our data (Fig. 7) with regard to the mixture $18:1_t/18:1_t$-glycerophosphocholine/16:0/16:0-glycerophosphocholine do not seem to be in agreement with a previous interpretation [2]. Our calorimetric scans both show a non-homogeneous transition peak and an equimolar mixture quenched from 0°C displays different regions of band patterns each with a characteristic periodicity (Fig. 8b). These findings support the view that in the diagram there must be a region in which solid-solid immiscibility occurs. The phase diagram (Fig. 7) obtained in the present study shows that this mixture is a borderline case of a system with a miscibility gap in the gel state. Rather small deviations from equilibrium may yield data that can be interpreted by a diagram with a totally miscible solid state [2].

We started this study because of the increasing number of phase diagrams being produced from probe studies. Although this technique is of great value in membrane research [16] one has to be very careful with the interpretation of the indirect information. The assumption that the probe, which is an impurity in the system, always reflects quantitatively the behaviour of the bulk phase can be questioned. It is therefore necessary to verify the phase diagrams by direct physical methods. The fact that two diagrams reported in this study yield different interpretations than those reported using ESR measurements makes one rather suspicious with respect to the reliability of the extremely complicated diagrams reported recently for other lipid mixtures [2]. We intend to verify also these kinds of mixtures by differential scanning calorimetry but

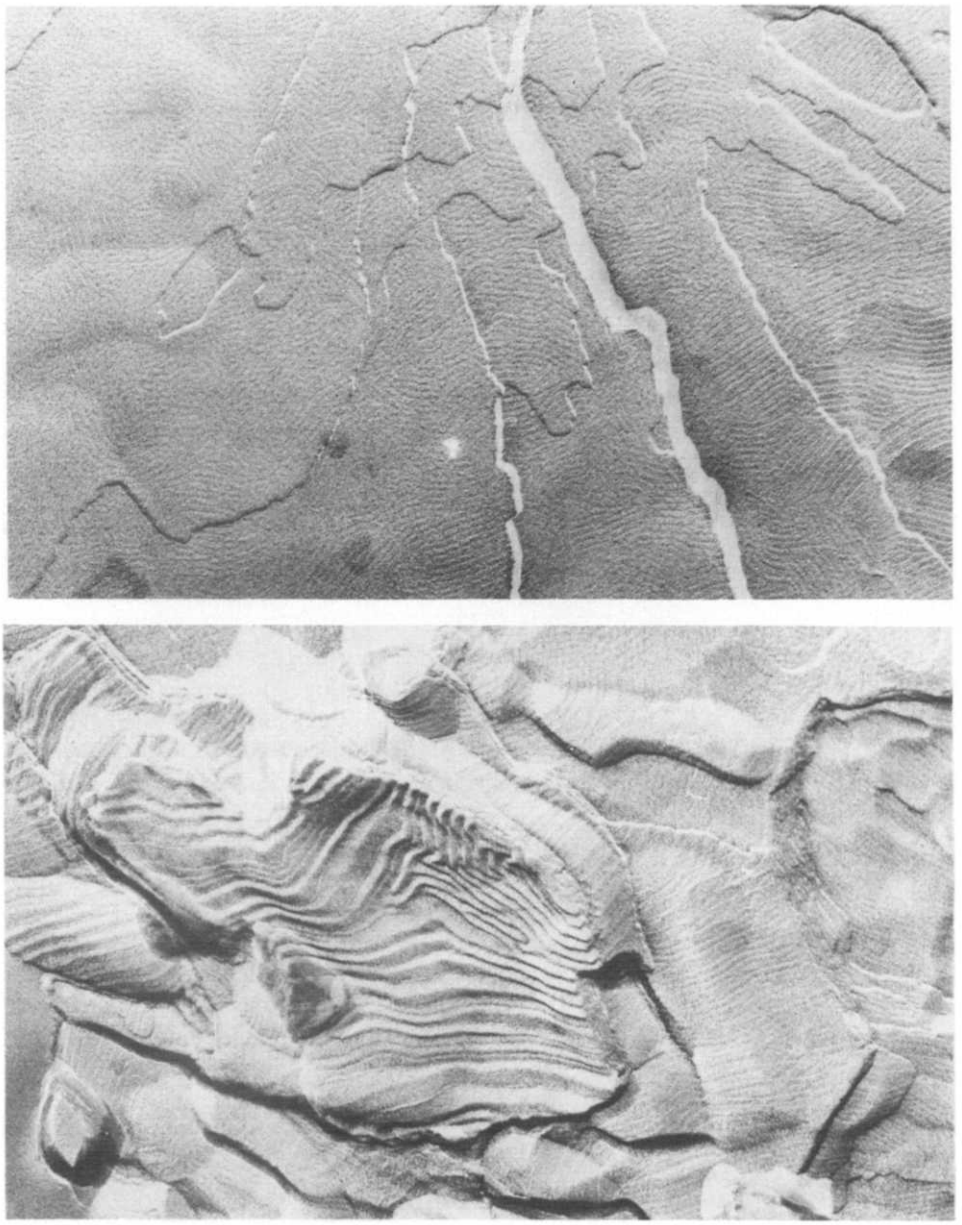

Fig. 8. Freeze fracturing electron micrographs. a. Equimolar mixture of $18{:}1_t/18{:}1_t$-glycerophosphocholine/14:0/14:0-glycerophosphocholine quenched from 0°C. Magnification 80 000×. b. Equimolar mixture of $18{:}1_t/18{:}1_t$-glycerophosphocholine/16:0/16:0-glycerophosphocholine quenched from 0°C. Magnification 80 000×.

we are aware that, with more complicated systems, phenomena like undercooling will create additional problems. Furthermore we want to investigate the gel to liquid crystalline transition in one of these systems at a higher level of accuracy. This can be done by using an adiabatic calorimeter in which we have

the possibility to scan with infinitely low speed. In this way also the pretransition can be incorporated in the phase diagram.

Acknowledgements

These investigations were carried out under the Auspices of the Netherlands Foundation of Chemical Research (S.O.N.) and with the financial aid from the Netherlands Organisation for the Advancement of Pure Research (Z.W.O.). We wish to thank Drs. E.J.J. van Zoelen for stimulating discussions and Dr. A.J. Verkleij (Institute of Molecular Biology, Utrecht) and J. Bijvelt for carrying out the freeze fracture experiments.

References

1 Shimshick, E.J. and McConnell, H.M. (1973) Biochemistry 12, 2351—2360
2 Wu, S.H.W. and McConnell, H.M. (1975) Biochemistry 14, 847—854
3 Lee, A.G. (1975) Biochim. Biophys. Acta 413, 11—23
4 Lentz, B.R., Barenholz, Y. and Thompson, T.E. (1976) Biochemistry 15, 4529—4537
5 Phillips, M.C., Ladbrooke, B.D. and Chapman, D. (1970) Biochim. Biophys. Acta 196, 35—44
6 Chapman, D., Urbina, J. and Keough, K.M. (1974) J. Biol. Chem. 249, 2512—2521
7 Blume, A. and Ackermann, Th. (1974) FEBS Lett. 43, 71—75
8 Mabrey, S. and Sturtevant, J.M. (1976) Proc. Natl. Acad. Sci. U.S. 73, 3862—3866
9 van Deenen, L.L.M. and de Haas, G.H. (1964) Adv. Lipid Res. 2, 168—363
10 de Kruijff, B., van Dijck, P.W.M., Demel, R.A. Schuijff, A., Brants, F. and van Deenen, L.L.M. (1974) Biochim. Biophys. Acta 356, 1—7
11 Ververgaert, P.H.J.Th., Verkleij, A.J., Elbers, P.F. and van Deenen, L.L.M. (1973) Biochim. Biophys. Acta 311, 320—329
12 Cullis, P.R. (1976) FEBS Lett. 70, 223—229
13 Oonk, H.A.J. (1970) J. Chem. Educ. 47, 227—229
14 Oonk, H.A.J., van Loo, T.J. and Vergouwen, A.A. (1976) Phys. Chem. Glasses 17, 10—12
15 Oonk, H.A.J. and Sprenkels, A. (1969) Rec. Trav. Chim. (Pays Bas) 88, 1313—1331
16 Keith, A.D., Sharnoff, M. and Cohn, G.E. (1973) Biochim. Biophys. Acta 300, 379—419